Large Area Transition-Edge Sensor Based Microcalorimeter with 40 meV Energy Resolution

C. Fink[1], S. Watkins[1], T. Aramaki[2], P. Brink[2], S. Ganjam[1], R. Mahapatra[3], N. Mirabolfathi[3], W. Page[1], R. Partridge[2], M. Platt[3], M. Pyle[1], B. Sadoulet[1], B. Serfass[1]

[1]Department of Physics, University of California, Berkeley, [2]SLAC National Accelerator Laboratory, [3]Department of Physics, Texas A&M

Introduction

Future low mass Dark Matter searches will require sensitivity to single optical phonons, corresponding to thresholds of about 100meV. This motivates the design of sensors with relatively large areas and excellent energy resolution. Transition-edge sensor (TES) based calorimeters are natural candidates for low mass DM detectors.

A tungsten TES with dimensions of $100\,\mu m \times 400\,\mu m \times 40$ nm and a T_c of 40mK was fabricated and studied to motivate its use with a 1cm^3 Si or Al_2O_3 target.

Small Signal Model for TES

The small signal current response of a voltage-biased TES [1] can be expressed as

$$Z(\omega) = R_{sh} + R_p + j\omega L + Z_{TES}(\omega) \quad (1)$$

Where

$$Z_{TES}(\omega) = R_0(1+\beta) + \frac{R_0\mathcal{L}}{1-\mathcal{L}}\frac{2+\beta}{1+\frac{j\omega\tau_0}{1-\mathcal{L}}} \quad (2)$$

The TES response to a Dirac delta impulse of power is

$$\frac{\partial I}{\partial P}(\omega) = \left[I_0\left(1-\frac{1}{\mathcal{L}}\right)\left(1+\frac{j\omega\tau_0}{1-\mathcal{L}}\right)Z(\omega)\right]^{-1} \quad (3)$$

where R_{sh} is the shunt resistance that converts the TES bias current into a voltage bias, R_0 is the resistance of the TES, L is the inductance of the SQUID, β is the current sensitivity, $\mathcal{L}$ is the loop gain, and $\tau_0 = C/G$ is the thermal time constant.

Experimental Setup

Two TES chips on single wafer studied in a dilution refrigerator with a base temperature of 15mK

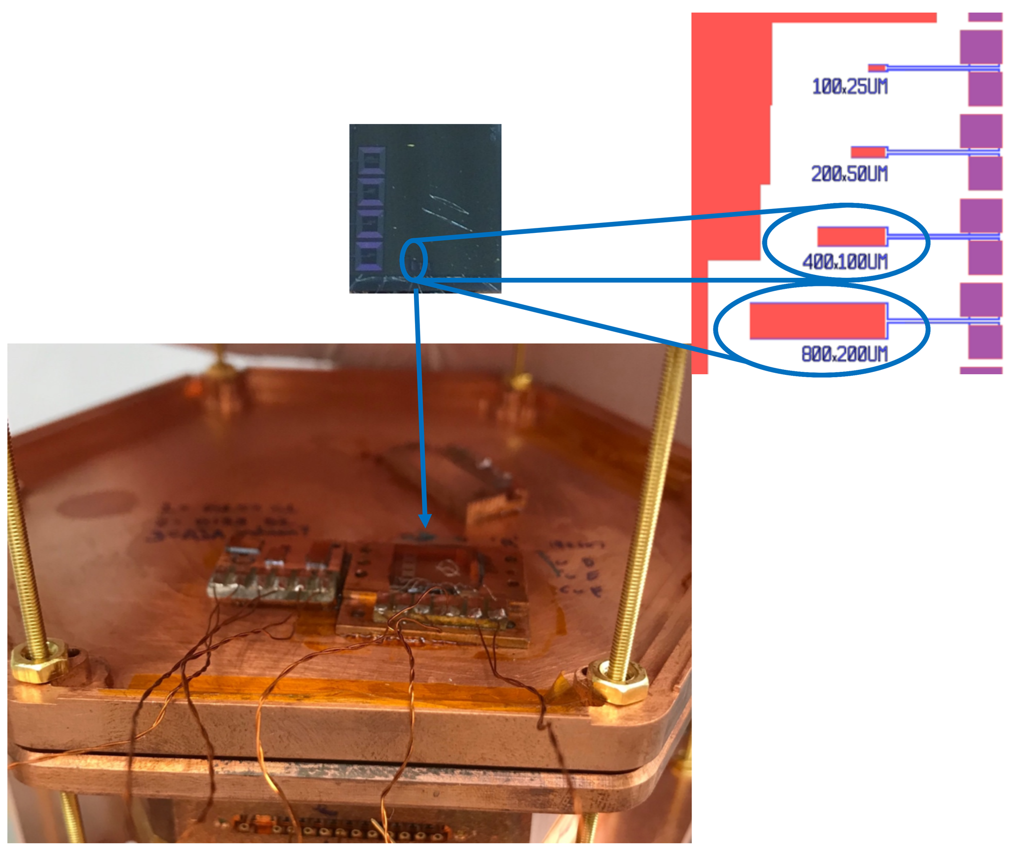

Figure 1. The experimental apparatus for characterizing the TES chip

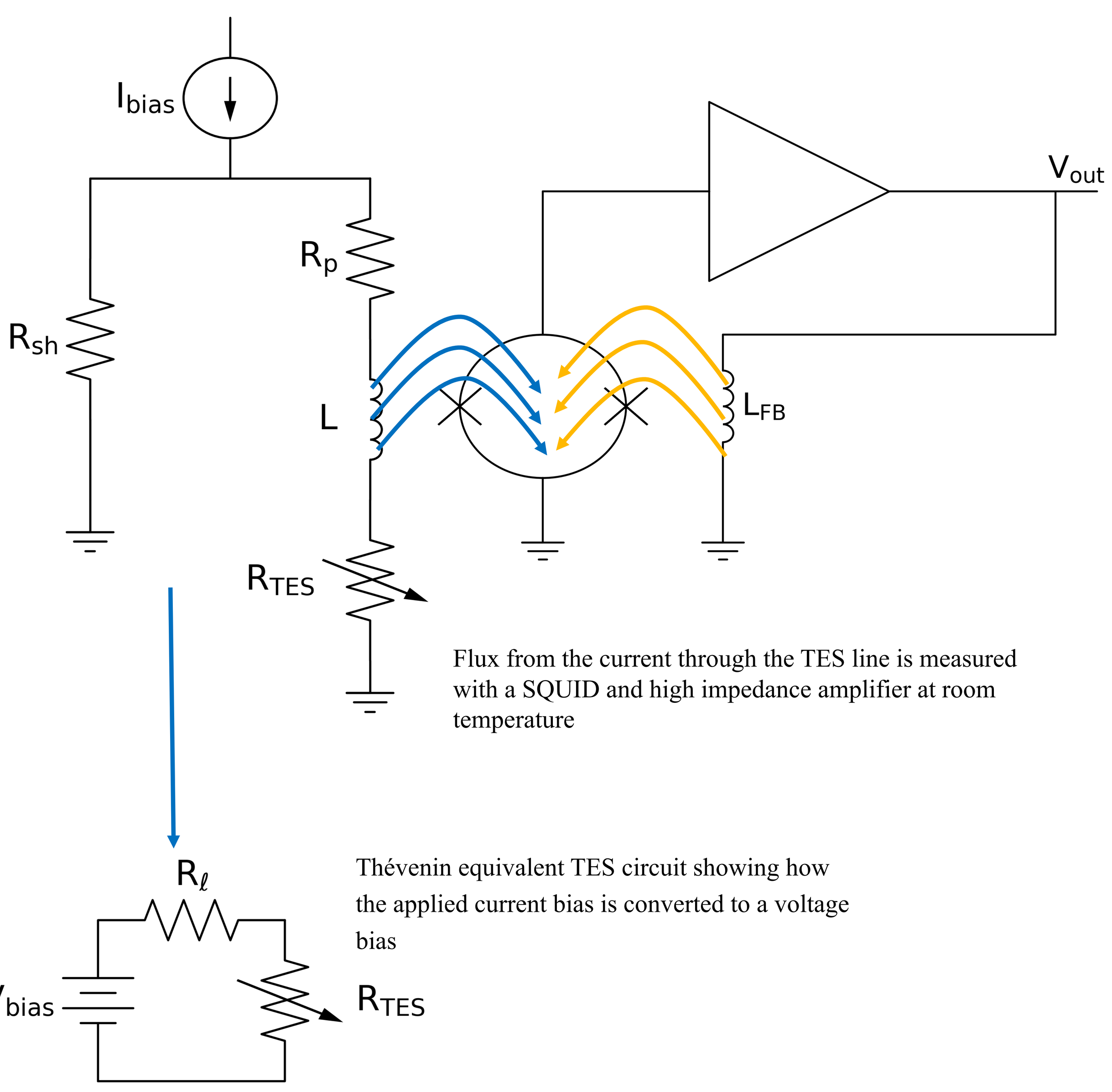

Figure 2. TES circuit and signal readout chain

Parameter Estimation

Measuring I_{TES} vs I_{bias} gives us the static properties of the TES

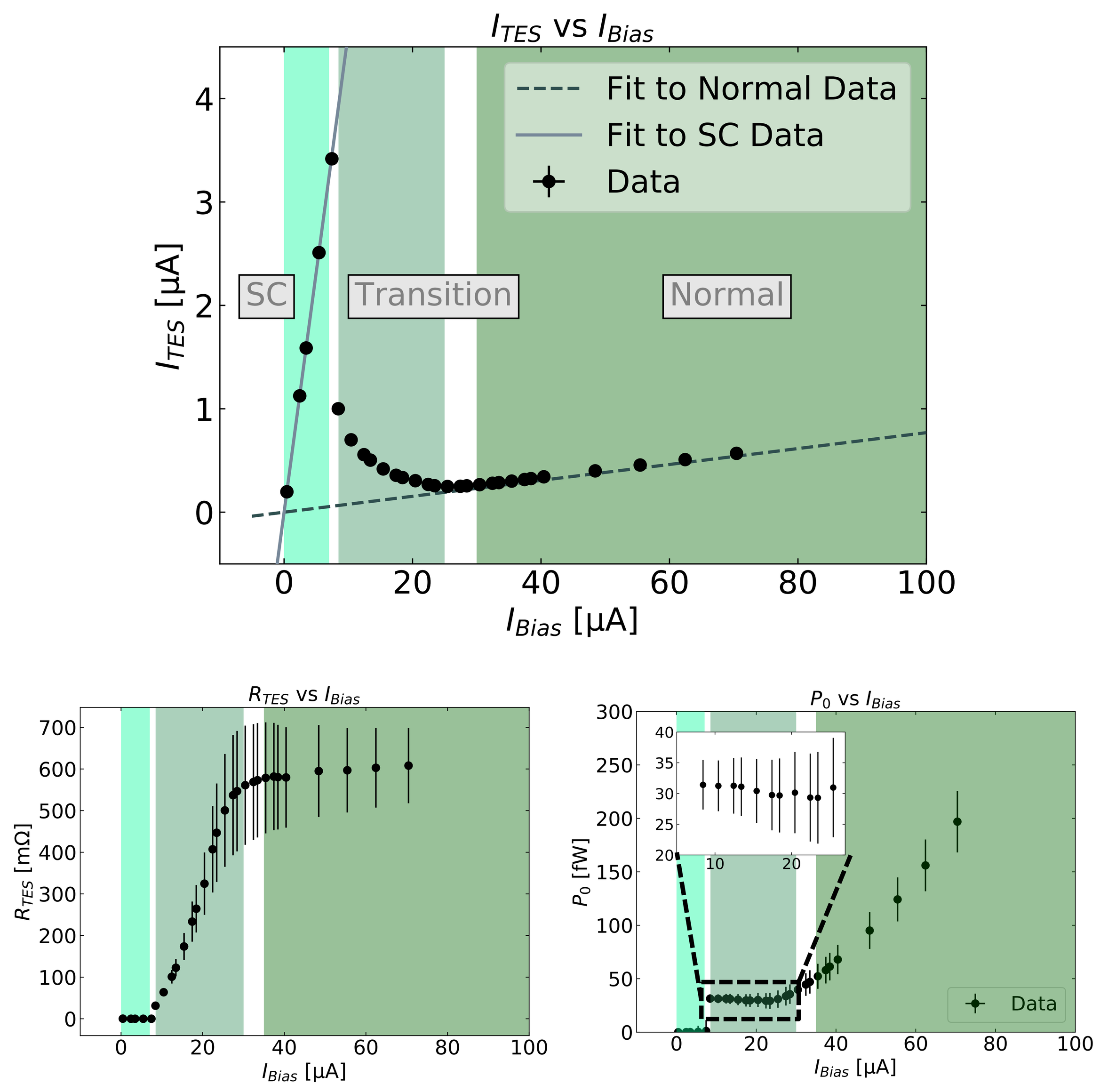

Figure 3. Top) I_{TES} vs I_{bias} curve, Left) R_{TES} vs I_{bias} curve, Right) Bias power vs I_{bias}

R_p [mΩ]	R_N [mΩ]	R_{Square} [Ω]	P_0[fW] (In equilibrium)
5.8 ± 0.6	640 ± 65	2.56 ± 0.26	31 ± 2

Studying the complex impedance (Eq. 1) gives us the dynamic properties of the TES: $\beta, L, \mathcal{L}, \tau_0$

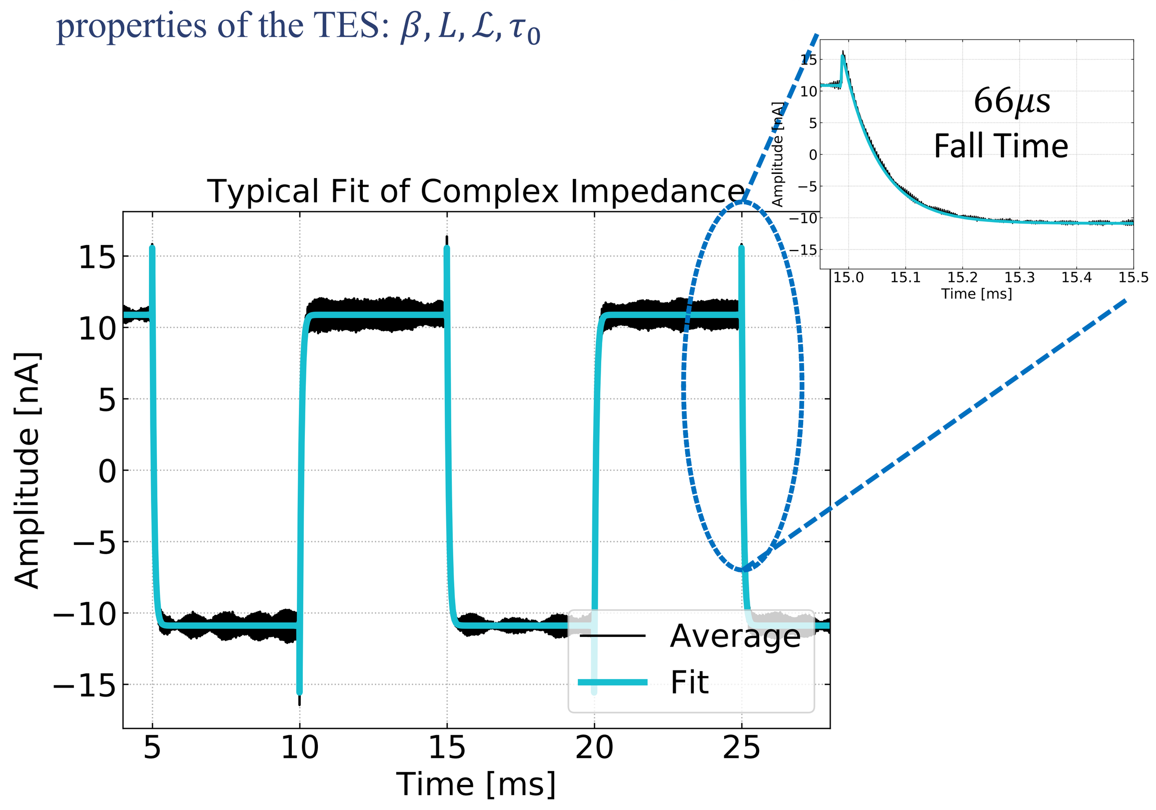

Figure 4. Typical fit of complex impedance data

Noise Modeling

We first estimate the effective temperature of the load resistance using the superconducting state data, then estimate the warm electronics noise to be the normal state PSD

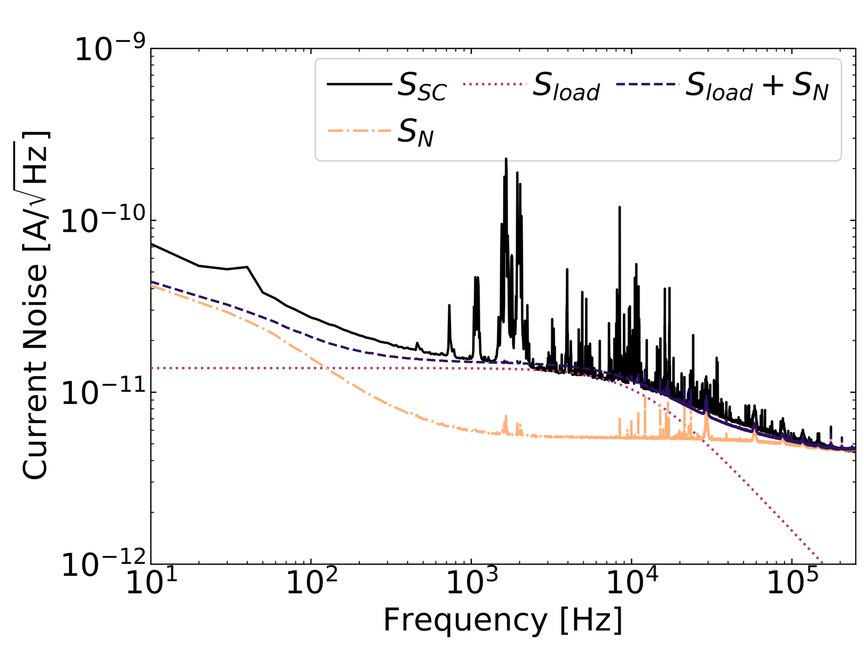

Figure 5. Normal (yellow) and Superconducting (black) state noise as well as an estimate of the Johnson noise from the load resistance

The fit to the complex impedance allows us to model the theoretical noise and to calculate the power to current transfer function in Eq 3.

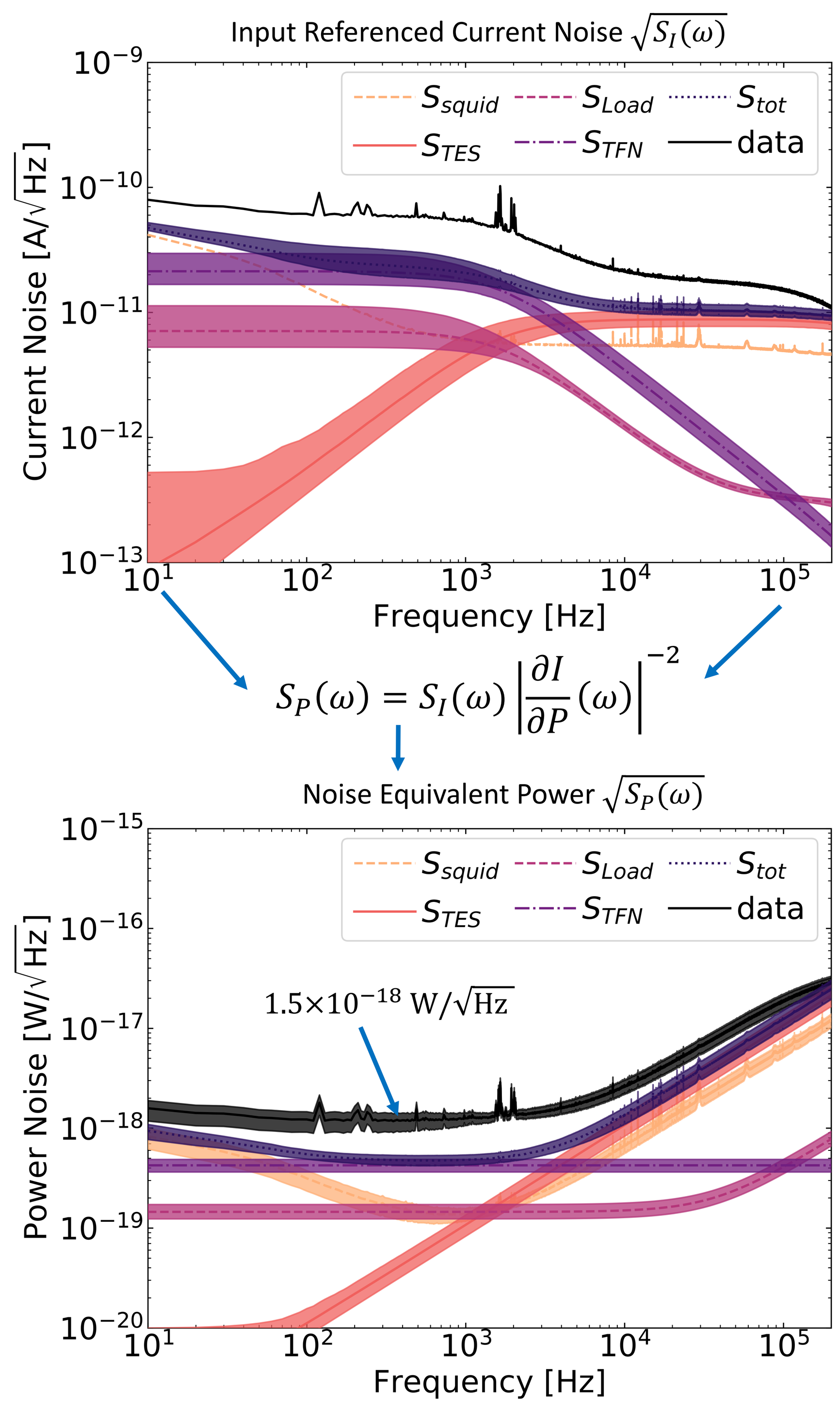

Figure 6. Top) Measured TES referenced current noise compared with noise model estimates. Bottom) Calculated Noise Equivalent Power compared with noise model estimates.

Energy Resolution

With the Noise Equivalent Power (NEP) measured, the expected energy resolution can be estimated as a function of the TES resistance R_0

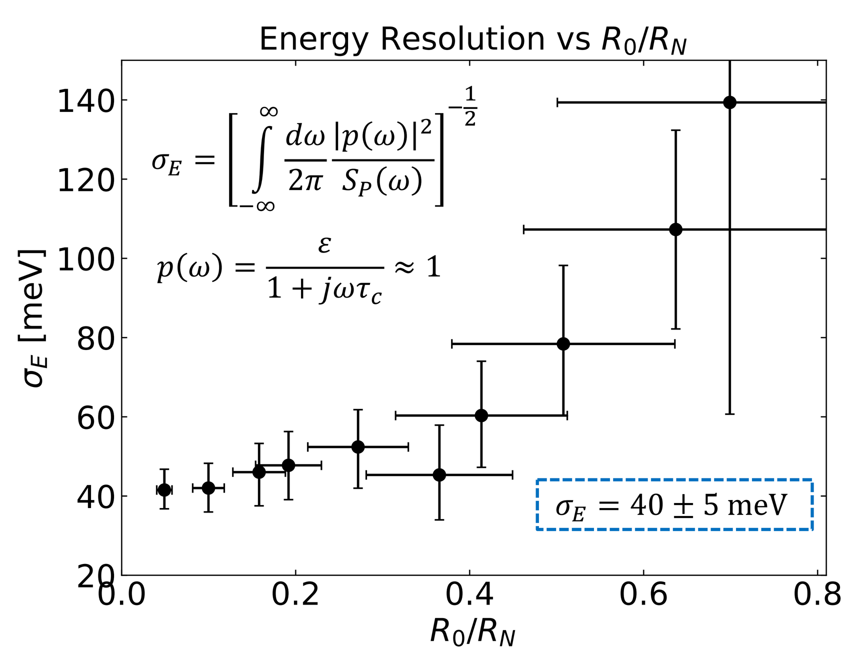

Figure 7. Estimated energy resolution as a function of TES resistance. We are assuming a collection efficiency $\varepsilon = 1$ and a phonon collection time τ_c of effectively zero.

We compare our result with other current state-of-the-art TESs in the table below. After normalizing for volume effects, our device shows world leading energy sensitivity.

TES	T_c [mK]	Volume [$\mu m \times \mu m \times nm$]	σ_E [meV]	$\frac{\sigma_E}{\sqrt{V}}\left[\frac{meV}{\sqrt{\mu m^3}}\right]$
W [2]	125	25×25×35	120	25.7
Ti [3]	50 100	6×0.4×56	47 47	128.2
MoCu [4]	110.6	100×100×200	295.4	6.6
TiAu [5]	106	10×10×90	48	16
TiAu [6]	90	50×50×81	~23*	1.6
W	40	100×400×40	40	1.0

*Estimated from NEP and response time

This result!

References

[1] Irwin K., Hilton G. () Transition-Edge Sensors. In: Enss C. (eds) Cryogenic Particle Detection. Topics in Applied Physics, vol 99. Springer, Berlin, Heidelberg

[2] A. J. Miller, S. W. Nam, J. M. Martinis, and A. V. Sergienko, Applied Physics Letters 83, 791 (2003).

[3] B. S. Karasik et. al., Applied Physics Letters 101, 052601 (2012).

[4] D. J. Goldie, A. V. Velichko, D. M. Glowacka, and S. Withington, Journal of Applied Physics 109, 084507 (2011)

[5] L. Lolli et. al., Applied Physics Letters 103, 041107 (2013)

[6] P. Khosropanah, T. Suzuki, M. L. Ridder, R. A. Hijmering, H. Akamatsu, L. Gottardi, J. van der Kuur, J. R. Gao, B. D. Jackson, "Ultra-low noise TES bolometer arrays for SAFARI instrument on SPICA," Proc. SPIE 9914, Millimeter, Submillimeter, and Far-Infrared Detectors and Instrumentation for Astronomy VIII, 99140B (19 July 2016)